

5G New Radio Sidelink Link-Level Simulator and Performance Analysis

Peng Liu

Georgetown University
Washington, DC, USA
National Institute of Standards and
Technology
Gaithersburg, Maryland, USA
peng.liu@nist.gov

Chen Shen*

Georgetown University
Washington, DC, USA
National Institute of Standards and
Technology
Gaithersburg, Maryland, USA
chen.shen@nist.gov

Chunmei Liu

National Institute of Standards and
Technology
Gaithersburg, Maryland, USA
chunmei.liu@nist.gov

Fernando J. Cintrón

National Institute of Standards and
Technology
Gaithersburg, Maryland, USA
fernando.cintron@nist.gov

Lyutianyang Zhang

University of Washington
Seattle, Washington, USA
lyutiz@uw.edu

Liu Cao

University of Washington
Seattle, Washington, USA
liuca@uw.edu

Richard Rouil

National Institute of Standards and
Technology
Gaithersburg, Maryland, USA
richard.rouil@nist.gov

Sumit Roy

University of Washington
Seattle, Washington, USA
sroy@uw.edu

ABSTRACT

Since the Third Generation Partnership Project (3GPP) specified 5G New Radio (NR) sidelink in Release 16, researchers have been expressing increasing interest in sidelink in various research areas, such as Proximity Services (ProSe) and Vehicle-to-Everything (V2X). It is essential to provide researchers with a comprehensive simulation platform that allows for extensive NR sidelink link-level evaluations. In this paper, we introduce the first publicly accessible 5G NR link-level simulator that supports sidelink. Our MATLAB-based simulator complies with the 3GPP 5G NR sidelink standards, and offers flexible control over various Physical Layer (PHY) configurations. It will facilitate researcher's exploration in NR sidelink with a friendly access to the key network parameters and great potential of customized simulations on algorithm developments and performance evaluations. This paper also provides several initial link-level simulation results on sidelink using the developed simulator.

CCS CONCEPTS

• **Computing methodologies** → **Simulation support systems**;
Simulation evaluation.

KEYWORDS

5G NR; Sidelink; Link-Level Simulator; Communication Range

*Now at Google.



This work is licensed under a Creative Commons Attribution International 4.0 License.

MSWiM '22, October 24–28, 2022, Montreal, QC, Canada

© 2022 Copyright held by the owner/author(s).

ACM ISBN 978-1-4503-9479-6/22/10.

<https://doi.org/10.1145/3551659.3559049>

ACM Reference Format:

Peng Liu, Chen Shen, Chunmei Liu, Fernando J. Cintrón, Lyutianyang Zhang, Liu Cao, Richard Rouil, and Sumit Roy. 2022. 5G New Radio Sidelink Link-Level Simulator and Performance Analysis. In *Proceedings of the International Conference on Modeling Analysis and Simulation of Wireless and Mobile Systems (MSWiM '22)*, October 24–28, 2022, Montreal, QC, Canada. ACM, New York, NY, USA, 10 pages. <https://doi.org/10.1145/3551659.3559049>

1 INTRODUCTION

In traditional cellular networks, devices first communicate with one or more base stations before reaching the other ends. On March 2015, the Third Generation Partnership Project (3GPP) specified Device-to-Device (D2D) communications in Release 12, which allow devices to connect directly to one another using Sidelink (SL). Since then, there have been extensive studies on SL communications. The technologies have advanced from 4G Long Term Evolution (LTE) to 5G New Radio (NR) [10], and the associated services have been extended from its original Proximity Services (ProSe) to Vehicle-to-Everything (V2X), and potentially other services that may benefit from D2D communications such as smart city ones.

Along the path of technology development, simulations play a significant role in algorithm design, protocol validation, and system performance evaluation. Accordingly, simulators at different levels have been developed and widely used, such as **i**) link-level simulation, which provides Physical Layer (PHY) performance evaluation in forms of Block Error Rate (BLER), Bit Error Rate (BER), or Frame Error Rate (FER), with accurate control over PHY parameters and environment conditions. Link-Level Simulators (LLSs) include MATLAB¹ LTE [14] and 5G [13] toolboxes, and Vienna¹ simulators [19]

for LTE and 5G; **ii**) system-level simulation, which focuses on the system performance evaluation in various system environment, such as scheduling strategy, frequency bands, and deployment configurations [16]. MATLAB LTE and 5G toolboxes and Vienna platform also have options for system-level simulation. A system-level simulator for 5G is also discussed in [9]; and **iii**) network-level simulation, which may take into account various network components, such as core network and radio access networks, and focuses on the performance of the network [9]. ns-3 [12] is a well known network simulator that have both LTE [18] and 5G [17] modules available.

Among these simulations, link-level simulations are widely used to simulate point-to-point communication links and PHY performance, and are often used to provide inputs to system-level simulations such as BLER curves. Specific to LTE and NR, there are two major suites of LLSs, both of which provide a rich set of PHY modules and are flexible to reuse. One suite comes from MathWorks. For LTE, MathWorks developed an LTE toolbox that supports Downlink (DL), Uplink (UL) and SL [14]. Accordingly, LLSs can be built using the tools provided. For SL in particular, MathWorks provides tools for Release 12 ProSe transmission mode 1 and mode 2, as well as Release 14 V2X transmission mode 3 and mode 4. Similarly, for NR, MathWorks developed a 5G toolbox that is compliant with 3GPP Release 15. However, while it supports both DL and UL, SL is not available at the time of writing. Another LLS suite comes from the Vienna Cellular Communications Simulators. This suite provides a variety of link-level and system-level simulators for both LTE and 5G NR [19]. Its 5G LLS supports DL and UL, and offers high flexibility in control over a wide variety of system parameters. However, as with MathWorks, there is lack of SL support. While there are other simulators mentioned in the literature [16] [11], to the best of our knowledge, there is no publicly accessible NR SL LLS yet.

To meet the simulation needs for the fast-developing NR SL technology and to fill the gap, in this paper we introduce the 5G NR SL LLS we developed for NR SL study [15]. The simulator is MATLAB based. Instead of developing NR SL LLS from scratch, we made use of the rich set of PHY modules from Vienna DL and UL LLS and MathWorks 5G toolbox, and developed NR SL specific features. The modules reused include general LLS software structure and some basic functionalities from Vienna LLS, and channel coding from MathWorks 5G toolbox. The NR SL features developed include, but not limited to, SL BWP and resource pool, SL slot format, data and control multiplexing and scrambling, SL layer mapping and precoding, and blind and feedback-based Hybrid Automatic Repeat Request (HARQ). In this paper, we also presents a variety of simulation results that proves the successful development of our simulator.

The simulator follows closely 3GPP 5G NR SL specifications, and has a highly flexible structure that is easy to adapt to various NR SL link-level simulations of interest. The simulator also keeps the branches of DL and UL LLS, so that it supports all DL, UL, and SL LLS. The current release focuses on one point-to-point NR SL and data transmissions. To the best of our knowledge, this simulator is the first 5G NR SL LLS that is publicly accessible.

¹Certain commercial equipment, instruments, or materials are identified in this paper in order to specify the experimental procedure adequately. Such identification is not intended to imply recommendation or endorsement by the National Institute of Standards and Technology (NIST), nor is it intended to imply that the materials or equipment identified are necessarily the best available for the purpose.

The rest of the paper is organized as follows. In Section 2 we introduce the simulator structure and supported features. In Section 3 we dive into NR SL features developed in detail. In Section 4 we present multiple simulation results using the simulator. And finally we present our concluding remarks in Section 5.

2 SIMULATOR STRUCTURE AND SUPPORTED FEATURES

The 5G NR SL simulator developed inherits the structure from Vienna 5G LLS, together with its general features [19]. Figure 1 illustrates the basic simulator structure. The simulator starts with loading a scenario profile, which contains the setup of the two User Equipments (UEs) and the link object that represents the connection between the two UEs. Transmission parameters are also specified, including but not limited to, antenna configurations, precoding matrix, channel coding scheme, waveform, channel model, and equalizer. Then a slot-by-slot simulation with a sweep parameter follows, and results of interest are stored. The results are then post-processed after the completion of a specified number of slots.

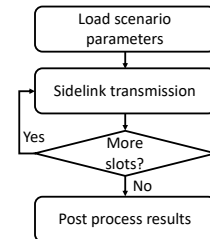


Figure 1: Basic Simulator Structure.

Specifically, instead of fixing Signal-to-Noise Ratio (SNR) as in most LLSs, Vienna 5G LLS fixes the transmit and noise power, and sets the path loss as an input parameter of the simulator [19]. We inherited this structure in the SL LLS. In addition, Vienna 5G simulator outputs throughput, BER, and FER as PHY performance metrics. While we kept them for the DL and UL branches, for SL, we output throughput, packet loss rate, and latency as performance metrics, and have plans to include BER and FER in future releases. Note that since the focus of link-level simulations is on physical layer, the latency here refers to the difference from the time a data packet is transmitted at the transmitter to the time it is received successfully at the receiver. It is a simplified version and does not include other delays such as processing delay. Monte Carlo simulations are then carried out and results are averaged over a certain number of channel, noise, and data realizations.

For SL in particular, Figure 2 illustrates the SL slot format with 2-symbol Physical Sidelink Control Channel (PSCCH), 2-symbol Physical Sidelink Shared Channel (PSSCH) Demodulation Reference Signal (DM-RS), and Physical Sidelink Feedback Channel (PSFCH). The slot formats corresponding to other settings are similar, and will be discussed in detail in Section 3. As the focus of the SL simulator in this release is on data channel, PSCCH and PSFCH are assumed to be error-free. That is, there is no loss on 1st-stage Sidelink Control Information (SCI1), Acknowledgements (ACKs), and Negative Acknowledgements (NACKs). Accordingly, dummy symbols with unit power are used to fill the Resource Elements (REs) for PSCCH and DM-RS. Meanwhile, Automatic Gain Control (AGC) and guard symbols are implemented per the 3GPP TS 38.211 [3].

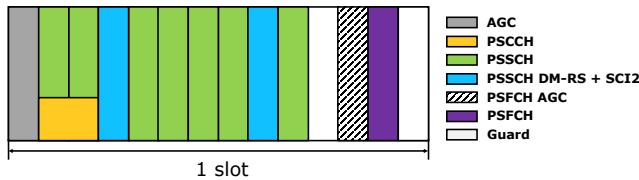


Figure 2: Generic 5G NR SL Slot Format.

Specific to PSSCH, which is the channel that carries data, Figure 3 illustrates at high level the processing chain at the transmitter and receiver sides. While the basic steps are similar to typical processing chains, there are multiple blocks that are specific to 5G NR SL.

First, in 5G NR SL, sidelink control information is carried in the Sidelink Control Information (SCI) messages, and SCI messages are transmitted in two stages, SCI1 and 2nd-stage Sidelink Control Information (SCI2). While SCI1 goes through PSCCH, SCI2 is multiplexed together with data and transmitted over PSSCH [6]. Nevertheless, the schemes applied to SCI2 and data are not always the same. One example is that SCI2 goes through Polar coding and Quadrature Phase Shift Keying (QPSK) modulation, while data goes through Low Density Parity Check (LDPC) coding and a selected modulation scheme from a set of Modulation and Coding Schemes (MCSs) [3]. This leads to SL specific processing, including separate coding, specific scrambling, separate constellation modulation, and specific layer mapping. The SL simulator implements these processes by closely following 3GPP, as shown in Figure 3, at both the transmitter side and the receiver side. Note that since the focus of this release is on data, the actual content of SCI2 is not significant. Dummy bits instead of the actual fields of SCI2 are used as SCI content, and these dummy bits then goes through the processing chain. Meanwhile, the simulator provides the flexibility to simulate both error-free SCI2 and error-prone SCI2, which allows evaluation of the impact of error-prone SCI2.

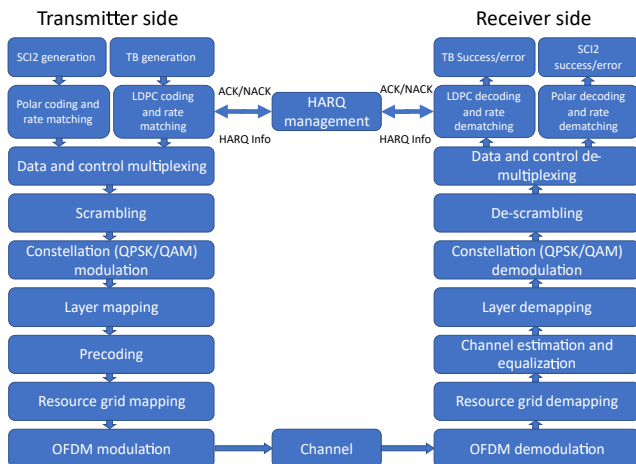


Figure 3: Transmitter and Receiver Processing Chain.

Second, as shown in Figure 2, the SL has specific resource grid. Meanwhile, 5G NR SL supports up to two layer spatial multiplexing, which allows reuse of the resource grid. The simulator supports this specific resource grid and the corresponding layer mapping.

Third, 5G NR SL supports both blind-based and feedback-based HARQ mechanisms, with a configurable and up to 32 maximum number of transmissions. While it is assumed that the feedback

channel is error-free and the content of PSFCH is not implemented, the simulator supports both PSFCH mechanisms following 3GPP [7], including feedback period and minimum gap.

The simulator also supports other 5G NR SL features, such as SL Bandwidth Part (BWP), resource pool, identity precoding matrix [8], and pathloss-to-range conversion. Table 1 summarizes features reused from Vienna 5G simulator and MathWorks, and features developed specifically for SL. In Section 3 we detail these features with a focus on the developed ones.

Table 1: Supported Features by the Simulator

| Inherited features | Developed features |
|----------------------------|---------------------------------|
| General Functionality | SL BWP and resource pool |
| Channel Coding | SL slot format |
| Channel Models | Data and control multiplexing |
| Channel Estimation | Data and SCI2 scrambling |
| Modulation | SL layer mapping and precoding |
| Equalization and Detection | error-free and error-prone SCI2 |
| | Blind- and feedback-based HARQ |
| | Pathloss-to-range conversion |

3 SIMULATOR FEATURES

The inherited features from Vienna NR UL and DL LLS and MathWorks 5G toolbox provide general functionalities to the NR SL implementation. To develop the NR SL LLS, however, the SL-specific configurations for these functionalities, as well as the SL-only features, still need to be comprehensively implemented. Such features are developed across different NR SL protocol stacks, including SL bandwidth part and resource pool in Radio Resource Control (RRC), blind- and feedback-based HARQ transmissions in Medium Access Control (MAC) and PHY, data and control multiplexing and scrambling, layer mapping and precoding, and SL slot structure in PHY. In addition, to facilitate the simulation and data acquisition, the selection between error-free and error-prone SCI2 is implemented, as well as some supported features, such as adaptive sweeping that automatically selects the SNR range for simulations, management of constants from 3GPP standards, and conversion between communication range and pathloss.

To ensure adequate functionalities, flexibility, and correctness of the SL simulator, the development of these SL features comply with 3GPP Release 16 specifications, while the structures of some parameters are modified to offload the configuration complexity without affecting their correctness. In the following subsections, we will introduce each of these SL feature in both functionality and its compliance with the 3GPP standards.

3.1 Sidelink Bandwidth Part and Resource Pool

3.1.1 Sidelink Bandwidth Part. The BWP for SL differs from those for UL or DL in that a UE can be configured with only one BWP for SL [7], whereas up to four UL or DL BWPs can be configured [3]. The SL BWP for a UE-specific NR SL communication is specified by the Information Element (IE) *SL-BWP-Config* in the RRC protocol [8]. It contains two major IEs:

- (1) *sl-BWP-Generic-r16*, which configures the generic SL BWP time and frequency resources, and
- (2) *sl-BWP-PoolConfig*, which configures the SL resource pool.

The structure of the SL BWP class, as well as its relation to the SL Resource Pool class, is illustrated in Figure 4.

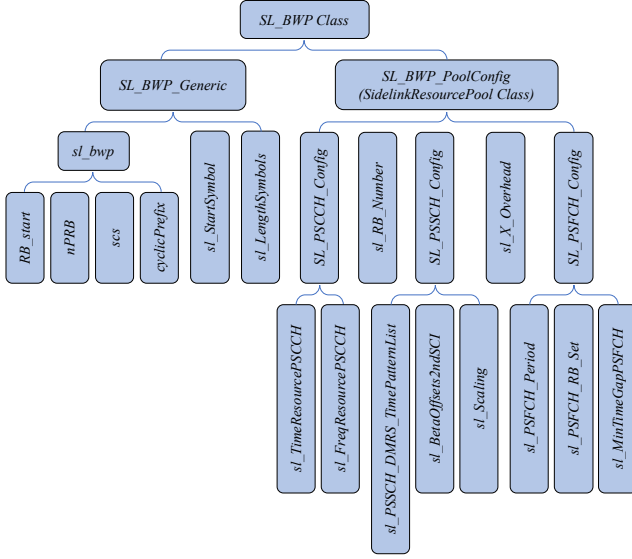


Figure 4: Structure of the *SL_BWP* class.

The Subcarrier Spacing (SCS) (*scs*) is related to the numerology (μ):

$$scs = 15 \times 2^\mu \text{ kHz}, \quad (1)$$

and *scs* can only be 15 kHz, 30 kHz, or 60 kHz in Frequency Range 1 (FR1), and 60 kHz or 120 kHz in Frequency Range 2 (FR2) [8].

The cyclic prefix (*cyclicPrefix*) can be normal or extended, which defines the number of Orthogonal Frequency-Division Multiplexing (OFDM) symbols in a slot (*nSymbol*). extended applies only when $\mu = 2$ [3]. *nSymbol* is 14 and 12 when *cyclicPrefix* is normal and extended, respectively. The index of the start symbol (*sl_StartSymbol*) and the length of the SL symbols in a slot (*sl_LengthSymbols*) can be configured by meeting the following condition:

$$sl_StartSymbol + sl_LengthSymbols \leq nSymbol. \quad (2)$$

To configure the start index of the Resource Blocks (RBs) (*RB_start*) and the number of RBs for the SL BWP (*nPRB*), we need to first acquire the maximum transmission bandwidth configuration in unit of RB (*maxRB*). *maxRB* is jointly determined by *scs* and the selected bandwidth, which is specified in Table 5.3.2-1 of [4] for FR1 or Table 5.3.2-1 of [5] for FR2. In addition, to ensure the configuration does not exceed *maxRB*, the following condition needs to be met:

$$RB_start + nPRB \leq maxRB. \quad (3)$$

3.1.2 Sidelink Resource Pool. The IE *SL_BWP_PoolConfig* specifies SL resource pool configuration. The SL resource pool updates every 10 240 ms, and provides configurations for PSCCH, PSSCH, and PSFCH. In the SL LLS, these configurations are stored using the *SidelinkResourcePool* class, as illustrated in Figure 4.

In each SL slot, two or three OFDM symbols can contain PSSCH, and the PSCCH can occupy 10, 12, 15, 20, or 25 Physical Resource Blocks (PRBs) [8]. The time and frequency resources allocated to PSCCH are defined by *sl_TimeResourcePSCCH* and *sl_FreqResourcePSCCH*, respectively.

In PSSCH, the number of OFDM symbols that contain DM-RS can be 2, 3, or 4, which is indicated by *sl_PSSCH_DMRS_TimePatternList*, *sl_TimeResourcePSCCH*, *sl_PSSCH_DMRS_TimePatternList*, and the number of OFDM symbols for PSSCH jointly determine the OFDM

symbols that contain PSSCH DM-RS, using Table 8.4.1.1.2-1 in [3]. *sl_BetaOffsets2ndSCI* corresponds to the length of the coded SCI2 modulation symbols [8], and *sl_Scaling* provides the upper bound ratio of the number of coded SCI2 modulation symbols over the total number of REs for PSSCH transmission. Both of them are used in the rate matching of the coded SCI2 bits [6].

In cases where feedback-based HARQ is enabled, *SL_PSFCH_Config* is configured. The PSFCH is transmitted on the dedicated SL slots with a periodicity of 1, 2, or 4 slots [8], which is configured by *sl_PSFCH_Period*. On reception of a PSSCH, the receiver waits for at least 2 or 3 slots of the resource pool before checking for an available PSFCH. This gap of slots is configured by *sl_MinTimeGapPSFCH*. The modulation symbols of the feedback information in the corresponding slot(s) and subchannel(s) are mapped to the RB set of *sl_PSFCH_RB_Set* [7]. As shown in Figure 6, when the PSFCH is to be transmitted, the OFDM symbol for PSFCH, as well as those for the PSFCH AGC that precedes it and the guard symbol that follows it, occupy the last three OFDM symbols of the SL slot.

It is worth mentioning that most of the configurations follow the 3GPP standards, while some parameters are simplified. For example, instead of having multiple configurations, each of *sl_PSSCH_DMRS_TimePatternList* and *sl_BetaOffsets2ndSCI* have only a single value. Also, in *sl_BetaOffsets2ndSCI*, we record the actual Beta offset value, instead of the lookup index for Table 9.3-2 of [7]. Another modification is that instead of subchannels, the frequency resources in the SL resource pool is configured based on the number of RBs *sl_RB_Number*. Such changes were made to simplify the configuration structure without loss of accuracy.

3.2 Sidelink Slot Format

As introduced above, an SL slot can contain 12 or 14 OFDM symbols in the time domain, depending on the cyclic prefix and SCS configurations. In frequency domain, (10 to 275) RBs can be configured, whereas the actual RB number is constrained by *nPRB* in SL BWP and eventually *sl_RB_Number* in SL resource pool. Each RB contains 12 subcarriers. The basic resource unit is an RE, which occupies one OFDM symbol in the time domain and one subcarrier in the frequency domain. An RE contains one modulation symbol for a physical channel or a reference signal.

An SL slot can contain 1) the physical channels of PSSCH, PSCCH, and PSFCH, and 2) the reference signals of DM-RS, Channel-State Information Reference Signal (CSI-RS), and Phase-Tracking Reference Signal (PT-RS). The PSSCH contains symbols of SCI2, data, and DM-RS, and the PSCCH contains symbols of SCI1 and DM-RS. In this simulator, we implemented the mapping of PSSCH, PSCCH, and PSFCH symbols for their corresponding elements, whereas the implementation of CSI-RS and PT-RS was left for future development.

In an SL slot, the first OFDM symbol starts at the symbol with index *sl_StartSymbol*, as specified in SL BWP. This symbol is used for AGC [10], and it is a duplication of the following OFDM symbol [3]. The PSCCH is mapped to the OFDM symbols starting at index *sl_StartSymbol* + 1, and its resources are specified by *sl_TimeResourcePSCCH* and *sl_FreqResourcePSCCH*. In the REs assigned to PSCCH, the symbols for the PSCCH DM-RS are mapped to the REs with index (k, l_0):

$$k = 4m + 1, m = 0, 1, 2, \dots, \quad (4)$$

complete such mapping, followed by duplicating the corresponding elements of PSCCH and PSSCH to the elements for AGC. At the receiver, after the OFDM demodulation, the modulation symbols are demapped by the *demap_PHY_Channels* function. Each individual function that *map_PHY_Channels* or *demap_PHY_Channels* calls can also be utilized individually when symbols for a specific physical channel or reference signal need to be modified or extracted.

In the LLS, the slot structures for the transmitter and receiver are initialized whenever the link between nodes are updated. The mapping of the physical channels and reference signals to the transmitter slot structure is implemented in the *sl_generateTransmitSignal* function after the modulations of the corresponding bit sequences. At the receiver, the OFDM demodulation is implemented in the *sl_processReceiveSignal* function, and its output is written to the RX slot structure matrix. The demapping functions in the *SL_Slot Structure* class are developed to demap either each physical channel or reference signal separately, or all of them can be demapped in one function. In the implementation, however, as we assume approximately perfect channel knowledge, only the demapping of SCI2 and data is implemented by modifying the original demapping functions of the Vienna simulator in order to comply with its channel estimation requirement.

3.3 Data and Control Multiplexing

Per 3GPP specification, in 5G NR SL, data and SCI2 are multiplexed together after channel coding and rate matching on the raw bit sequences. The multiplexed bits are then scrambled with the scrambling sequence. The output sequence of the data and control multiplexing process is completed by concatenating the coded SCI2 bits with the coded data bits, and its format is determined by *nLayer*.

If the coded SCI2 and coded data bit sequences have the lengths of m and n , and

$$\text{codedSCI2Bits: } b_0 b_1 \dots b_{m-1},$$

$$\text{codedDataBits: } d_0 d_1 \dots d_{n-1},$$

the multiplexed bit sequence (*multiplexedBits*) is shown in 1) Figure 8a when the number of data streams (*nStreams*) is 1, and 2) Figure 8b when *nLayer* is 2. Considering the SCI2 messages for both layers are identical in the two-layer scenario, and the modulation scheme for SCI2 is QPSK, every two groups of two coded SCI2 bits are interleaved by a group of $[-1, -1]$, which, during scrambling processing, are then replaced by the group of two scrambled bits before it.

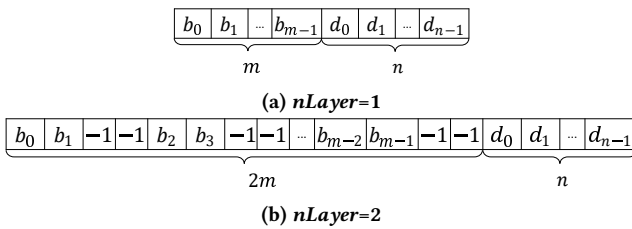


Figure 8: Multiplexed bit sequence for different *nLayer* values.

At the receiver, the demultiplexing of data and control follows the descrambling procedure, and the demultiplexed SCI2 and data bits then go through rate recovery and channel decoding. It is worth noting that as two SCI2's are received in the 2-layer scenario, to improve the decoding performance, we keep both SCI2s for rate recovery and channel decoding.

The data and control multiplexing and demultiplexing are implemented by the *sl_multiplex* and *sl_demultiplex*, and they process the corresponding data in *sl_generateTransmitSignal* and *sl_processReceiveSignal*, respectively.

3.4 PSSCH Scrambling

The scrambling on PSSCH is performed between the multiplexed sequence and the scrambling sequence $c(n)$ before modulation. The format of the scrambled sequence differs with *nLayer*.

The multiplexed sequence before scrambling is shown in Figures 8a and 8b for one-layer and two-layer scenarios, respectively. When scrambling is performed, each bit in b and d scrambles with the corresponding bit in $c(n)$:

$$\begin{aligned} \tilde{b}_n &= (b_n + c(n)) \bmod 2, \\ \tilde{d}_n &= (d_n + c(n)) \bmod 2. \end{aligned} \quad (8)$$

In a one-layer scenario, the scrambled sequences of \tilde{b} and \tilde{d} are concatenated in the same format as in Figure 8a. The scrambled format is shown in Figure 9a. In a two-layer scenario, however, each $[-1, -1]$ group shown in Figure 8b is replaced by the group of two scrambled SCI2 bits before it. The scrambled format is shown in Figure 9b. The PSSCH scrambling is realized by the function *sl_scrambling*.

At the receiver, the PSSCH descrambling follows the demodulation of the received symbols. The descrambling reverses the procedures for scrambling and outputs the descrambled sequence with the same format as in Figure 8a in the one-layer scenario. In the two-layer scenario, the descrambled SCI2 bits for Layer 2 are saved for decoding, instead of being replaced by $[-1, -1]$ groups. It is important to note that, as the demodulated sequence is in the form of Log-Likelihood Ratio (LLR), the descrambling is also performed by converting the corresponding scrambling sequence to the LLR form.

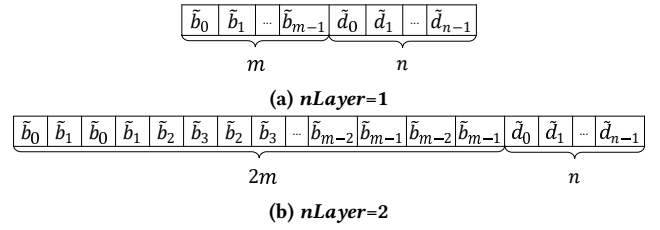


Figure 9: Scrambling on PSSCH for different *nLayer* values

The scrambling sequence $c(n)$ is generated by two length-31 Gold sequences [3]:

$$c(n) = (x_1(n + 1600) + x_2(n + 1600)) \bmod 2, \quad (9)$$

where $x_1(n)$ is initialized by

$$x_1(n) = \begin{cases} 1 & n = 0, \\ 0 & n = 1, 2, \dots, 30, \end{cases} \quad (10)$$

and

$$\sum_{i=0}^{30} x_2(i) \cdot 2^i = c_{\text{init}}. \quad (11)$$

c_{init} is related to the 24-bit Cyclic Redundancy Check (CRC) on PSCCH p [3], [6]:

$$\begin{aligned}
c_{\text{init}} &= 2^{15} N_{\text{ID}} + 1010, \\
N_{\text{ID}} &= N_{\text{ID}}^{\text{X}} \bmod 2^{16}, \\
N_{\text{ID}}^{\text{X}} &= \sum_{i=0}^{L-1} p_i \cdot 2^{L-1-i}, L = 24.
\end{aligned} \tag{12}$$

In the simulator, the generation of scrambling sequence is completed by the function `sl_scrambleSequence`. p and the length of the scrambling sequence are the inputs to the function. As the coded sequences of SCI2 and data share the scrambling sequence with the same c_{init} but different lengths, $c(n)$ is generated with the length of the longer of these two sequences. The first 31 bits in each of $x_1(n)$ and $x_2(n)$ are generated with bitwise operation in binary to avoid the computation complexity in decimal.

3.5 Sidelink Layer Mapping and Precoding

Different from LTE SL where no spatial multiplexing is supported, NR SL supports MIMO transmission up to two layers. Accordingly, layer mapping and precoding will be implemented after modulation on the scrambled PSSCH bit sequence. The layer mapping procedure splits the modulated symbol sequence according to n_{Layer} , and the precoding scales the symbols in each layer and maps each layer to its corresponding antenna port.

In a one-layer scenario with modulation order Q for data bits, the first $m/2$ symbols of the modulated symbol sequence S are SCI2 symbols S^b , and the last n/Q symbols are data symbols S^d . S is mapped to a single layer, and the precoding has an identity precoding matrix of $W = 1$. Figure 10a illustrates an example of the procedures from scrambled bit sequence to a one-layer precoded symbol sequence, with the data modulation of 16 Quadrature Amplitude Modulation (QAM) ($Q = 4$).

In a two-layer scenario, the first m symbols of S are SCI2 symbols S^b , where S_k^b with $k = 0, 2, \dots, m-2$ are mapped to Layer 1, and those with $k = 1, 3, \dots, m-1$ are mapped to Layer 2. The last n/Q symbols are data symbols S^d , where S_k^d with $k = 0, 2, \dots, n/Q-2$ are mapped to Layer 1, and those with $k = 1, 3, \dots, n/Q-1$ are mapped to Layer 2. The layer mapped sequence is then multiplied with the identity precoding matrix W :

$$\begin{aligned}
Z &= WS, \\
W &= \begin{bmatrix} 1 & 0 \\ 0 & 1 \end{bmatrix}.
\end{aligned} \tag{13}$$

The two-layer procedures from scrambled bit sequence to precoded symbol sequence are shown in Figure 10b, with the data modulation of QPSK ($Q = 2$).

In the LLS, layer mapping and precoding are implemented in the `sl_generateTransmitSignal` function, and the precoding matrix is defined in the `SidelinkScenario` script.

3.6 Error-Free and Error-Prone SCI2

In physical layer design and performance evaluation, the performance of control signaling transmission, such as PSCCH and SCI2, is often an interesting topic for researchers. In addition, in link-to-system mapping, there are often various requests on BLER-to-SNR mapping, such as control only, data only, or integrated control and data. For this purpose and to provide flexible options, our SL simulator provides the options of 1) error-free SCI2, which separates the data collection and processing of SCI2 from decoding of a Transport

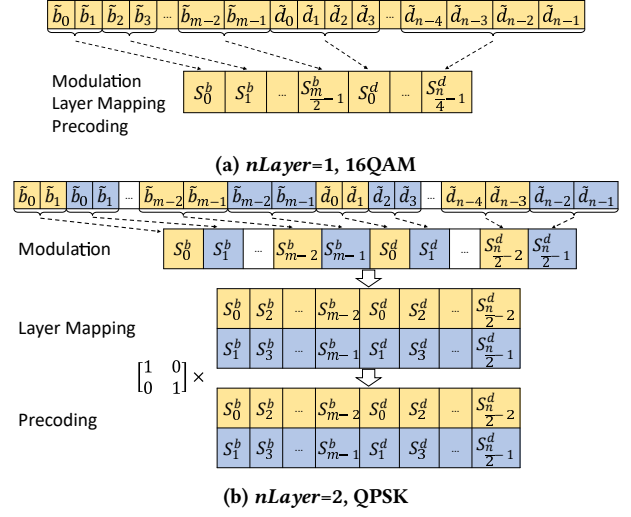


Figure 10: SL layer mapping and precoding for one-layer and two-layer scenarios.

Block (TB), and 2) error-prone SCI2, where a TB cannot be decoded properly if the associated SCI2 is not received correctly.

In the error-free SCI2 scenario, the decoding of a data transmission is under the assumption that the SCI2 is decoded without an error. The data transmission in each slot is decoded, and the BLER is recorded by summarizing the decoding results of each TB transmission(s). The BLER of SCI2 transmission is also recorded separately, and its BLER is calculated by summarizing the decoding result of SCI2 in each slot. The error-free SCI2 scenario can be enabled in the `SidelinkScenario` script.

When the error-prone SCI2 scenario is enabled, if the decoding of SCI2 in a slot returns an error, the decoding of this TB transmission is skipped and automatically recorded as erroneous. The decoding error of SCI2 transmissions in this scenario is still recorded for each slot, whereas the decoding error of TB transmission(s) reflects the error from both SCI2 and TB transmissions.

3.7 Blind-Based and Feedback-Based HARQ

To increase reliability of TB transmissions, for unicast, 5G NR SL supports both blind-based HARQ and feedback-based HARQ, and the maximum number of transmissions is configurable and up to 32 [8]. In blind-based HARQ, transmitter UE transmits one TB for a certain number of times without requiring any HARQ feedback. Whereas in feedback-based HARQ, transmitter UE retransmits the TB after receiving a NACK or no response after a predefined time, up to the configured maximum number of transmissions. Apparently, on one hand, feedback-based HARQ can prevent unnecessary retransmissions that would otherwise waste SL resources and increase the channel load. On the other hand, feedback-based HARQ requires feedback that occupies SL resource and could potentially increase latency. In our LLS, blind-based or feedback-based HARQ is set as one scenario parameter, which is used later in the resource pool object.

Per 3GPP [7], HARQ feedback for a TB sent on a PSSCH in a resource pool is carried on a PSFCH within the same resource pool. Resources for PSFCH can be (pre-)configured periodically with a period of $N = 1, 2, \text{ or } 4$ slot(s), i.e., there is a slot with PSFCH every N

slots [8]. To disable the HARQ feedback for a specific TB, the value of 0 can be set to the HARQ feedback enabled/disabled indicator field in the corresponding SCI2 [6]. To disable the HARQ feedback for all SL transmissions in the resource pool, no resources for PSFCH are configured [8]. In the LLS, PSFCH configuration is realized in the resource pool object. Since the focus of the LLS is one point-to-point link, HARQ feedback is not enabled/disabled at the TB level, but rather at the resource pool level.

In addition, to accommodate the processing delay at the receiver UE, in 3GPP [8], a time gap $sl\text{-}MinTimeGapPSFCH$ between the PSSCH and the PSFCH is configured in the time domain, with a single value of 2 or 3 per resource pool. The receiver UE transmits the PSFCH in a first slot that includes PSFCH resources and is at least $sl\text{-}MinTimeGapPSFCH$ slots in the resource pool after a last slot of the PSSCH reception. In the LLS, this time gap is implemented in the resource pool object, and is also used in the resource allocation mechanism to ensure the minimum time gap between the associated PSSCH and PSFCH.

Given that the focus of the LLS is one point-to-point link instead of scheduling algorithms, the LLS implements a simple resource allocation mechanism. For blind-based HARQ, all transmissions of one TB are transmitted in consecutive slots. For feedback-based HARQ, note that the number of symbols available to PSSCH differs between a slot with PSFCH and a slot without PSFCH (Figure 5 and 6). This means that the sizes of the TBs that these two types of slots can hold are different. In the LLS, if the initial transmission of one TB is on a slot with PSFCH, all its retransmissions are scheduled in slots with PSFCH, and vice versa.

To avoid waste of resources while waiting for HARQ feedbacks, 3GPP further allows multiple simultaneous outstanding TBs [2], and HARQ process IDs are used to identify the TBs. Moreover, different copies of the same TB are combined at the receiving UE based on their redundancy versions, and each redundancy version is generated by shifting the starting position of the bit sequence after LDPC encoding [6]. In the LLS, an SL HARQ entity is developed to manage HARQ processes and redundancy versions, as illustrated in Figure 11. As shown in the figure, the active HARQ process is selected based on whether its associated slot type (with or without PSFCH) matches the current slot and whether the minimum time gap between its associated PSSCH and PSFCH is satisfied. If both requirements are met, the process that waited longer in the buffer is selected. After the active HARQ process is selected, the next redundancy version of the associated TB is transmitted.

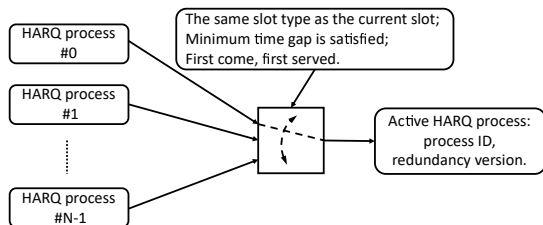


Figure 11: HARQ Management

3.8 Pathloss-to-Range Conversion

Communication range is one major topic in wireless communications and of special interest since the beginning of D2D communications. In this context, communication range refers to the maximum

distance between a transmitter and a receiver such that the transport block transmitted could be received with an error probability not exceeding the Target Loss Rate (TLR). By using the pathloss models defined by 3GPP, the pathloss-to-range conversion feature allows our SL LLS to give range numbers directly from link-level simulations.

Channel models for D2D are defined in 3GPP specifications for ProSe under LTE [1], which include three deployment scenarios: Outdoor-to-Outdoor (O2O), Outdoor-to-Indoor (O2I), and Indoor-to-Indoor (I2I). In each of the O2O and O2I scenarios, both Line-of-Sight (LOS) and Non-Line-of-Sight (NLOS) cases are specified. In the I2I scenario, only NLOS case is considered, and an additional penetration loss can be added when more than one obstacle is involved. This gives six deployment scenarios in total. Figure 12 provides the distance-vs-pathloss curves at band n14 for all these six scenarios.

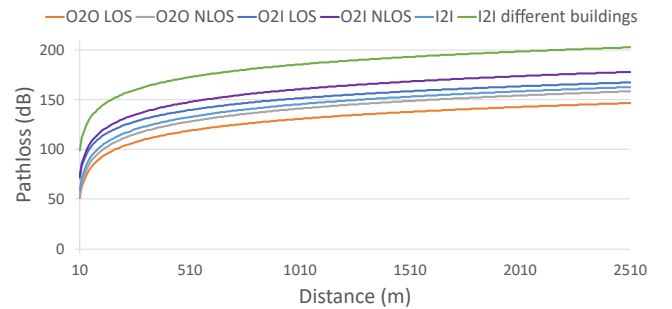


Figure 12: LTE D2D pathloss models for different deployment environment.

As shown in Figure 13, the pathloss-to-range conversion feature contains a major function `getDistanceFromPathloss`. It returns the corresponding distance according to the specified values of pathloss and deployment environment. When the function is executed for the first time, `getDistanceFromPathloss` calls `generateChModelTables` to generate the lookup tables for the six scenarios. These lookup tables are generated by `O2O_pathloss_3gpp`, `O2I_pathloss_3gpp`, and `I2I_pathloss_3gpp`. When a lookup table is used in `getDistanceFromPathloss` and the pathloss value happens to be absent, interpolation is used to estimate the corresponding distance,

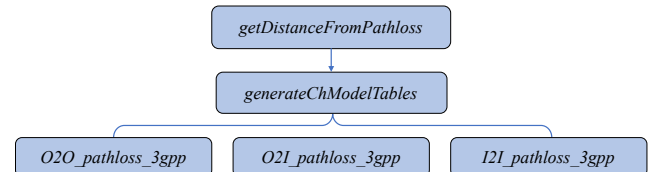


Figure 13: Functions for the pathloss-to-range conversion.

4 SIMULATION RESULTS

In this section, we demonstrate that the simulator can be flexibly used to evaluate the impact of different parameters under various research topics. Additionally, we present several simulation results using our SL LLS. The examples of simulations we use are performed on one point-to-point link at public safety band n14, which uses center frequency 795 MHz and Frequency Division Multiplexing (FDD), with one power class 3 transmitter UE (transmit power 23 dBm) and one receiver UE. Unless mentioned otherwise, other simulation parameters are set as follows. Numerology is set to 0, O2O

LOS pathloss model is used with Additive White Gaussian Noise (AWGN) channel, and noise figure is set to 9 dB. 20 PRBs are allocated for data transmissions and MCS corresponding to Channel Quality Indication (CQI) 1 is deployed. For HARQ, PSFCH is disabled, and maximum number of transmissions is set to 1. Also, error-free SCI2 and perfect channel knowledge are assumed.

4.1 Error-Free SCI2 vs Error-Prone SCI2

As introduced in Section 3.6, to support the study of control signaling transmission and to facilitate link-to-system mapping, our SL LLS supports both error-free SCI2 and error-prone SCI2. In this simulation, we use our SL LLS to investigate the impact of error-prone SCI2 on TB decoding. We implemented this simulation set by flipping the error-prone SCI2 option for all the CQI indexes of Table 5.2.2.1-2 in [2]. The resulting BLER curves are shown in Figure 14.

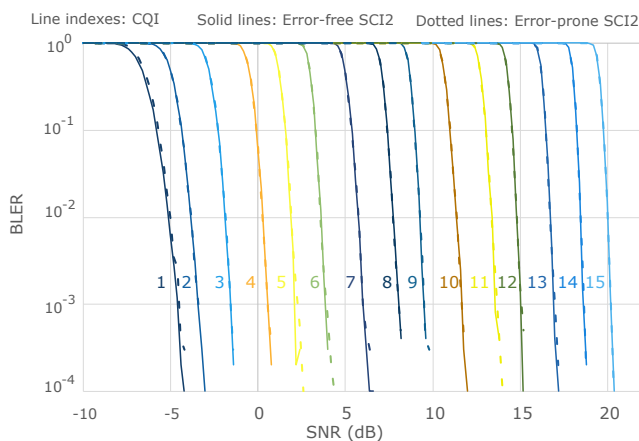


Figure 14: BLER curves for error-free SCI2 and error-prone SCI2.

In Figure 14, each pair of curves with the same color represents the TB BLERs of one MCS, with solid lines and dotted line representing the error-free SCI2 scenario and the error-prone SCI2 scenario, respectively. It can be observed that, for each pair, the solid line is slightly to the left side of the dotted line, indicating a better performance in the error-free SCI2 scenario. Nevertheless, the difference is barely visible. It indicates that under the same channel condition, the impact of error-prone SCI2 decoding on the decoding of a TB is negligible. This is consistent with the design of control signaling, which uses polar coding and QPSK, and is required to be more robust due to its importance.

4.2 Impacts of Numerology

5G NR introduces flexible numerology (μ) to support a variety of services with different performance requirements. This changes the resource grid in both time and frequency domains. For example, in frequency domain, the SCS is 15 kHz for $\mu = 0$ and 30 kHz for $\mu = 1$. As we set $n_{PRB} = 20$, the bandwidth when $\mu = 1$ is twice than that when $\mu = 0$. Meanwhile, in time domain, the time duration of a slot is 1 ms for $\mu = 0$ and 0.5 ms for $\mu = 1$. In this simulation, we explore the impacts of numerology on the required SNR, communication range, throughput, and latency for both $\mu = 0$ and 1, at a TLR of 0.5 %.

Figure 15 shows that at a TLR of 0.5 %, the required SNRs for $\mu = 0$ and 1 are the same. The SNRs can be converted to pathloss

values by combining transmitting power, noise figure, bandwidth, and operating temperature. As $\mu = 1$ has a larger SCS and bandwidth, its signal power is more dispersed.

From the function introduced in Section 3.8, a shorter communication range is expected. This is consistent with Figure 15.

In terms of throughput, note that both cases share the same n_{PRB} but SCS is doubled in case of $\mu = 1$. The resource utilized in case of $\mu = 1$ is hence doubled, and the throughput is therefore expected to be around twice as that for $\mu = 0$. This derivation is reflected in Figure 15. Likewise, as a TB is decoded in the same slot as it is transmitted, using our simplified version of latency without considering other delays, the latency for $\mu = 1$ is expected to be around half of that for $\mu = 0$, which is also reflected in Figure 15.

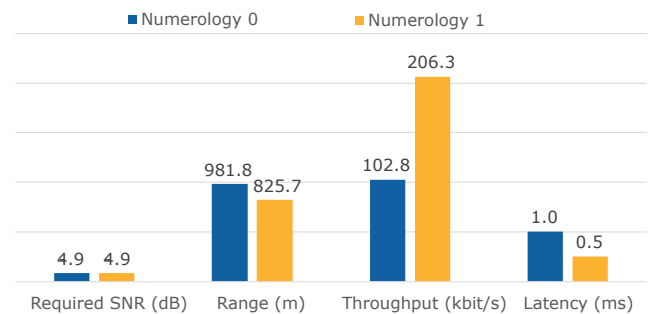


Figure 15: Impacts of numerology on required SNR, range, throughput, and latency (numerology 0 and 1, at TLR = 0.5 %).

The above simulation data shows how numerologies influence the performance metrics towards different directions, which further validates the goal of introducing numerology in 5G to support a variety of service needs.

4.3 Range under Enhanced NR Sidelink HARQ Mechanism

Since the start of D2D communications, communication range has been one major topic of interest. While LTE SL supports blind-based HARQ with four mandatory transmissions, 5G NR SL supports both blind-based and feedback-based HARQ, and allows up to 32 transmissions. This brings a great potential to improve D2D communication range. In this simulation, we use our SL simulator to study range under different HARQ configurations.

For this purpose, for both blind-based and feedback-based HARQ, we set maximum number of transmissions to be 1,4,8,16, and 32, respectively. In the feedback-based HARQ simulation, we enable PSFCH transmission with a PSFCH period of 4. The corresponding range can be calculated from the BLER curves at a TLR of 0.5 %. The results for both blind-based and feedback-based HARQ are plotted in Figure 16.

The range curve in Figure 16 shows a significant improvement in range values with increasing number of transmissions, for both blind-based and feedback-based HARQ. This is consistent with our expectation, as a higher number of (re)transmissions increases the TB decoding success rate. The link can hence tolerate a higher path loss, which leads to a longer range.

However, more transmissions would also lead to a higher latency. We hence plot latency curves in Figure 16, which clearly shows a significant increase in latency. The latency can be as high as around 140 ms, which would fail many applications. Also, as retransmission

in feedback-based HARQ only happens after a corresponding PSFCH is received, its latency is expected to be significantly higher than the latency for blind-based HARQ, especially when the maximum number of transmissions is high. Figure 16 shows that the latency for feedback-based HARQ can be as high as 122 ms longer than that of blind-based HARQ.

This data shows that NR SL enhanced HARQ can indeed improve communication range significantly. However, a careful design is required to balance other performance metrics, such as latency, in order to meet various service needs.

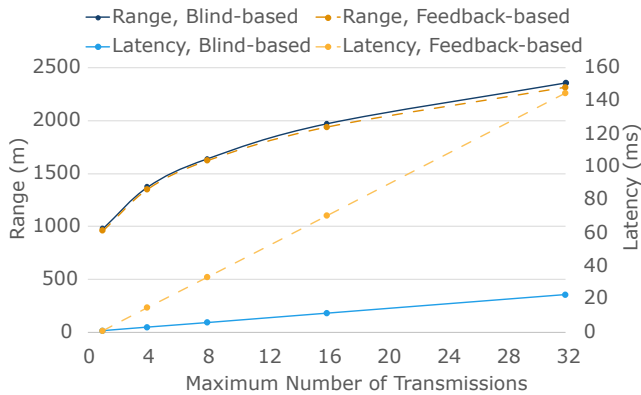


Figure 16: Range and latency for blind-based HARQ and feedback-based HARQ, at TLR = 0.5 %.

5 CONCLUSION

In this paper we introduced the 5G NR sidelink link-level simulator we developed, which is available on [15]. The simulator follows closely the 3GPP specifications on NR sidelink. It supports a variety of NR sidelink features, such as sidelink BWP and resource pool, sidelink slot format, data and control multiplexing, data and SCI2 scrambling, sidelink layer mapping and precoding, blind- and feedback-based HARQ, and pathloss-to-range conversion. It is highly modularized and adaptive to different link-level simulations of interests. In this paper we also used our sidelink simulator to study a couple of research topics, including error-free vs error-prone SCI2, impacts of numerology, and communication range under enhanced HARQ mechanism, which further validated the simulator. To the best of our knowledge, this simulator is the first 5G NR sidelink link-level simulator that is publicly accessible.

The current release of the simulator focuses on one point-to-point sidelink with FDD and data transmissions with partial implementation of control and feedback channel, and the performance metrics are mainly BLER, throughput and latency. In our future releases we plan to extend it to include full implementation of control channel and feedback, as well as other performance metrics such as BER and FER. As link-level simulation at V2X frequency bands is another motivation in the future development, Time Division Multiplexing (TDD) transmission will also be developed. In addition, we plan to pursue PHY abstraction to feed the link-level data into system-level simulations.

ACKNOWLEDGMENTS

The authors thank Tom Henderson (University of Washington) for insightful technical discussions and guidance throughout the project, and Jean-Aicard Fabien (National Institute of Standards and Technology) for providing timely support on 3GPP specifications and their developments.

REFERENCES

- [1] 3GPP. 2014. *Study on LTE device to device proximity services; Radio aspects (Release 12)*. Technical Report (TR) 36.843. 3rd Generation Partnership Project (3GPP). <https://portal.3gpp.org/desktopmodules/Specifications/SpecificationDetails.aspx?specificationId=2544> Version 12.0.1.
- [2] 3GPP. 2020. *NR; Physical layer procedures for data (Release 16)*. Technical Specification (TS) 38.214. 3rd Generation Partnership Project (3GPP). <https://portal.3gpp.org/desktopmodules/Specifications/SpecificationDetails.aspx?specificationId=3216> Version 16.3.0.
- [3] 3GPP. 2021. *NR; Physical channels and modulation (Release 16)*. Technical Specification (TS) 38.211. 3rd Generation Partnership Project (3GPP). Version 16.6.0.
- [4] 3GPP TS38.101-1. 2021. *3rd Generation Partnership Project; Technical Specification Group Radio Access Network; NR; User Equipment (UE) radio transmission and reception; Part 1: Range 1 Standalone*. Standard. 3GPP.
- [5] 3GPP TS38.101-2. 2021. *3rd Generation Partnership Project; Technical Specification Group Radio Access Network; NR; User Equipment (UE) radio transmission and reception; Part 2: Range 2 Standalone*. Standard. 3GPP.
- [6] 3GPP TS38.212. 2021. *3rd Generation Partnership Project; Technical Specification Group Radio Access Network; NR; Multiplexing and channel coding*. Standard. 3GPP.
- [7] 3GPP TS38.213. 2021. *3rd Generation Partnership Project; Technical Specification Group Radio Access Network; NR; Physical layer procedures for control*. Standard. 3GPP.
- [8] 3GPP TS38.331. 2021. *3rd Generation Partnership Project; Technical Specification Group Radio Access Network; NR; Radio Resource Control (RRC) protocol specification*. Standard. 3GPP.
- [9] Sangjin Cho, Seungyeob Chae, Minjoong Rim, and Chung G. Kang. 2017. System level simulation for 5G cellular communication systems. In *2017 Ninth International Conference on Ubiquitous and Future Networks (ICUFN)*. 296–299. <https://doi.org/10.1109/ICUFN.2017.7993797>
- [10] Fernando Cintron, David Griffith, Chunmei Liu, Richard Rouil, Yishen Sun, Jian Wang, Peng Liu, Chen Shen, Aziza Ben Mosbah, and Samantha Gamboa Quintiliani. 2021. Study of 5G New Radio (NR) Support for Direct Mode Communications. <https://doi.org/10.6028/NIST.IR.8372>
- [11] Wang Donglin, Raja R. Sattiraju, Qiu Anjie, Sanket Partani, and Hans D. Schotten. 2019. Methodologies of Link-Level Simulator and System-Level Simulator for C-V2X Communication. <https://doi.org/10.48550/ARXIV.1907.04693>
- [12] Thomas R. Henderson, Mathieu Lécage, and George F. Riley. 2008. Network simulations with the ns-3 simulator. In *Sigcomm Demo*.
- [13] The MathWorks Inc. 2022. *5G Toolbox User's Guide*. https://www.mathworks.com/help/pdf_doc/5g/5g Ug.pdf
- [14] The MathWorks Inc. 2022. *LTE Toolbox User's Guide*. https://www.mathworks.com/help/pdf_doc/lte/lte Ug.pdf
- [15] National Institute of Standards and Technology and University of Washington. 2022. *New Radio Sidelink Simulator*. <https://www.nist.gov/services-resources/software/new-radio-sidelink-simulator>
- [16] University of Surrey. 2022. *Link Level Simulator*. <https://www.surrey.ac.uk/institute-communication-systems/facilities/link-and-system-level-simulators>
- [17] Natale Patriciello, Sandra Lagen, Biljana Bojovic, and Lorenza Giupponi. 2019. An E2E Simulator for 5G NR Networks. <https://doi.org/10.48550/ARXIV.1911.05534>
- [18] Giuseppe Piro, Nicola Baldo, and Marco Miozzo. 2011. An LTE Module for the ns-3 Network Simulator. In *Proceedings of the 4th International ICST Conference on Simulation Tools and Techniques (Barcelona, Spain) (SIMUTools '11)*. ICST (Institute for Computer Sciences, Social-Informatics and Telecommunications Engineering), Brussels, BEL, 415–422.
- [19] Stefan Pratschner, Bashar Tahir, Ljiljana Marijanovic, Mariam Mussbah, Kiril Kirev, Ronald Nissel, Stefan Schwarz, and Markus Rupp. 2018. Versatile mobile communications simulation: the Vienna 5G Link Level Simulator. *EURASIP Journal on Wireless Communications and Networking* 2018, 1 (20 Sept. 2018), 226. <https://doi.org/10.1186/s13638-018-1239-6>